FinJeHeW Finnish Journal of eHealth and eWelfare

SCIENTIFIC PAPERS
VERTAISARVIOITU
KOLLEGIALT GRANSKAD
PEER-REVIEWED
www.tsv.fi/tunnus

Skull fracture detection for point-of-care diagnostics using microwave technique

Mariella Särestöniemi[1,2,3], Daljeet Singh[1,3], Jarmo Reponen[1], Mikael von und zu Fraunberg[4,5], Teemu Myllylä[1,3,4,6]

[1] Research Unit of Health Science and Technology, Faculty of Medicine, University of Oulu,, Finland; [2] Centre for Wireless Communications, Faculty of Information Technology and Electrical Engineering, University of Oulu, Finland; [3] InfoTech Oulu, University of Oulu, Finland; [4] Medical Research Center Oulu, Oulu University Hospital and University of Oulu, Finland; [5] Oulu University Hospital, Finland; [6] Optoelectronics and Measurements, Faculty of Information Technology and Electrical Engineering, University of Oulu, Finland

Mariella Särestöniemi, Dr. (Tech), PhD, Research Unit of Health Sciences and Technology, PO Box 5000, FI-90014 University of Oulu, FINLAND. Email: mariella.sarestoniemi@oulu.fi

Abstract

The possibility to detect severity of skull fractures outside the hospital already in the accident location would be a promising eHealth application. Such a point-of-care type of device would smoothen the patients' path to the treatment after the accident. Additionally, frequent and safe monitoring of the healing process of skull fractures in smaller healthcare centers, as a new telemedicine solution, would enable early detection of potential problems. Microwave technique has shown significant potential for portable monitoring devices since it enables safe, low-cost, and high accuracy detectors. This paper has three research objectives: (1) to investigate the potential of microwave techniques for detecting common skull fracture types using antennas embedded in a small, portable monitoring device, (2) to evaluate optimal frequency ranges for skull fracture detection, and (3) to examine the impact of scalp thickness on fracture detectability. The research is carried out using electromagnetic simulation software with human head models resembling different scalp thicknesses and flexible antennas operating at 2.5–10 GHz. In the evaluations, scattering parameters are analyzed with the head models both with and without the fractures. The evaluation results show that different types of skull fractures can be detected with microwave technique. Fractures cause differences in scattering parameters ranging from 2 dB to 12 dB, depending on the type of fracture. The most optimal frequency ranges for detection are 3–5 GHz and 9 GHz. The thickness of the scalp impacts the detectability of skull fractures, yet fractures remain detectable even with the model with thicker scalp. These findings support the potential of microwave technique for developing portable, point-of-care devices for timely and precise skull fracture pre-diagnosis and frequent monitoring of the healing process. This approach particularly benefits young children, for whom conventional screening methods may pose more significant challenges.

Keywords: diagnostic technique, monitoring, point-of-care diagnostics, rural nursing, skull fracture, telemedicine

Introduction

Skull fractures typically result from substantial cranial impacts, such as encountered during falls, car accidents, or sports injuries. Timely and precise diagnosis of skull fractures is crucial for preventing complications and improving treatment outcomes [1–2]. Therefore, early assessment of fracture severity, evaluation of treatment options, and determination of hospitalization needs are important. A point-of-care skull fracture detector would be particularly beneficial to fasten the patients' path to the treatment after the accident [3]. Additionally, a readily accessible and safe method for monitoring the healing process of skull fractures would be invaluable for early identification of potential complications [2].

There are various types of skull fractures, which are illustrated in Figure 1a. Each fracture has distinct characteristics and implications:

A) Linear fracture: This is the most common skull fracture type, characterized by a single fracture line without bone displacement. Commonly thin linear fractures do not require any operations, just monitoring that the healing process starts properly. [2]

B) Depressed fracture: In this type, a portion of the skull is pushed inward toward the brain, potentially causing additional brain injury. This fracture type commonly requires surgery. [2]

C) Diastatic fracture: This type involves the separation of the cranial sutures, which are the joints between the bones of the skull. Usually, diastatic fractures are at least 4 mm wide. Necessity for surgery depends on the severity of the fracture. [2]

D) Basal (Basilar) fracture: This involves a break in the bones at the base of the skull, often affecting areas around the eyes, ears, and nose. [2]

Skull fractures are conventionally diagnosed/monitored by Digital Radiography (DR), Computed Tomography (CT), Magnetic Resonance Imaging (MRI) and ultrasound [1–3]. DR is available even in small hospitals with an x-ray department, but it fails to detect small fractures and requires skill to interpret complicated fractures. CT scans provide quick, highly detailed, three-dimensional images of the skull, making it easier to locate even minor fractures. However, CT scans are costly, and both DR and CT involve exposure to ionizing radiation, which can be harmful with repeated use. MRI scans use magnetic fields and radio waves to provide excellent details of soft tissues, which is useful for assessing adjacent brain injuries. MRIs are more time-consuming and expensive than CT scans and not always available in all facilities. Ultrasound imaging uses sound waves, eliminating radiation exposure and hence it is safe for frequent monitoring. Portable ultrasound devices can be used bedside, which is especially beneficial in monitoring for children's skull fractures [4]. However, ultrasound is less effective in detecting skull fractures compared to CT and MRI, and its accuracy depends on the operator's skill. [1–3]

Microwave technique has shown significant potential in detecting abnormalities in the tissues [5–7], including bone fractures and skull fractures [8–17]. Studies by Redzwan et al. [8] and Lee et al. [9] demonstrated the technique's potential for real-time bone healing monitoring. The microwave technique has shown high accuracy even for minor fractures [10–11]. This technique has also been applied to monitor skull fracture healing post-surgery using a layered head model to analyze skull healing through time domain shifts [12]. It has been also shown that skull healing progression could be monitored by analyzing variations in reflected pulse amplitudes [13–16]. A detailed investigation into the detection of linear skull fractures using microwaves

was presented in [17]. The findings demonstrated the capability of microwaves to detect fractures as narrow as 1 mm in realistic models and to monitor the healing process of these fractures. However, the study in [17] was limited to linear skull fractures, excluding other types of skull fractures.

The main advantages of the microwave technique over existing skull fracture monitoring methods include its safety, even with frequent use, and its cost-effectiveness. The technique offers high-resolution detection capability and can be implemented as a small, portable point-of-care device. Additionally, the possibility for both contact and non-contact sensing provides a significant benefit over other methods, as it allows for flexible application scenarios. Furthermore, the device is user-friendly, with accuracy that does not depend on the expertise of the examiner, unlike ultrasound techniques. This makes it particularly suitable for widespread use also outside clinical settings where specialized training may not be available. Table 1 presents the various properties of existing skull fracture detection techniques and the microwave technique, facilitating an easy comparison between these methods.

Research aims and research questions

This study aims to investigate the potential of microwave technology in detecting the most common types of skull fractures using an antenna system that could be integrated into a portable device. The secondary aim is to study the most optimal frequencies for skull fracture detection with different skull fracture types. The third aim is to study the impact of scalp thickness on detectability of fractures.

The research questions (RQ)s of this study are:

RQ1. How different skull fracture types affect the scattering parameters (S-parameters) of antennas located in the vicinity of the fracture?

RQ2: What are the most optimal frequencies to detect different skull fractures?

RQ3: How much tissue scalp thickness affects the detectability of the skull fractures?

Table 1. Comparison between existing skull fracture detection techniques and microwave technique.

Technique	Output	Resolution Temporal	Resolution Spatial	Cost	Device size	Contact / Non-contact sensing	Safe with frequent scans
MRI+ variations	3D image	Low	High	High	Large	Yes	No
CT	3D image	Low	High	High	Large	Yes	No
Ultrasound	3D image	High	Low	Relatively Low	Small	No	Yes
Microwaves	S-parameters, images	High for detecting differences in S-parameters, but relatively low for imaging	High (depending on frequency), for detecting differences in S-parameters, but relatively low for imaging	Low	Small; most promising technique for a handheld/wearable device	Both possible	Yes

Scenarios and methods

In this section, research scenarios and methods are described. First, the basic idea and the principle of skull fracture detection utilizing microwave technique is introduced. Dielectric properties of head tissue and corresponding fracture model tissues are presented. Finally, the simulation model and antennas are presented.

Basic principle of bone fracture detection with microwaves

Detecting skull bone fractures with microwaves works by exploiting the differences in the dielectric properties of bone, blood, and connective tissue [18]. These differences help to distinguish between fresh fractures (modelled with blood) and those that are in the healing process (connective tissue) [19]. Table A1, presented in Appendix, details the dielectric properties (relative permittivity and conductivity) of head tissues, blood, and connective tissue at various frequencies [18]. It also highlights the differences between bone and blood at these frequencies. Notably, the disparity in dielectric properties between bone and blood/connective tissue varies with frequency. These variations clearly affect signal propagation within the skull, as the boundaries between materials with different dielectric properties cause additional diffractions in the propagating signal [20]. The differences in the radio channel characteristics can be detected with sensitive receivers, which then analyzes the data and estimates the presence of abnormalities [5–7].

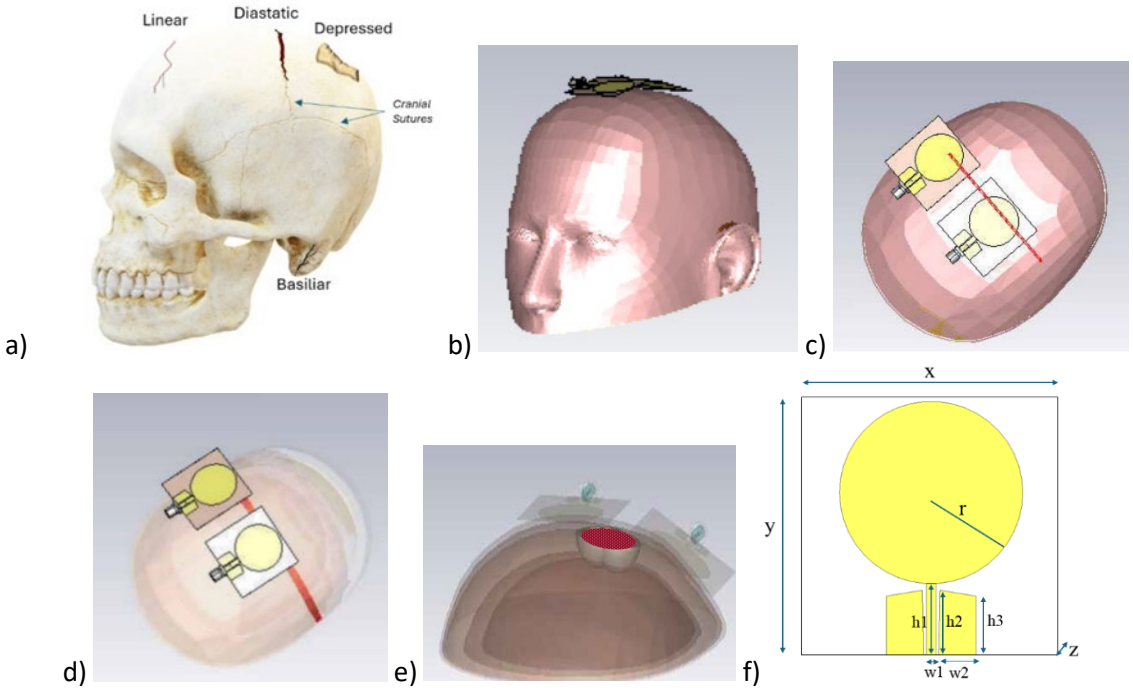

Figure 1. a) The illustration of the most typical skull fractures: linear, diastatic, depressed and basilar fractures, b) the human head model used in the simulations, c) linear fracture model, d) diastatic fracture model, e) depressed fracture model, f) antenna model used in the simulations.

Research methods

Simulations: human model and fracture modeling

Microwave propagation can be approximated with electromagnetic simulations software. In our study, we utilized the Dassault Simulia CST Studio Suite [21] and its homogeneous human model, as depicted in Figure 1b. The homogeneous head model was modified to create two multilayer head models by incorporating separate head tissue layers with realistic dimensions for the skin, fat, bone, dura, and brain. The first human head model (Model 1) corresponds to the head with thinner scalp thickness: with skin layer 1.5 mm and fat layer 1.5 mm. The second head model (Model 2) corresponds to the thicker scalp: skin layer 2 mm and fat layer 3 m. In both cases the thickness of the skull layer is 6 mm and dura 1 mm. The models' tissue thicknesses are summarized in Table 2.

The primary motivation for developing these layered head models stemmed from the observations in [17] that CST's Hugo head model featured an excessively thick fat layer in the upper part of the head. Such a thick fat layer above the skull leads to overly pessimistic simulation results in skull fracture detection studies.

The most common fracture models: linear, diastatic and depressed fracture models were created for the head models as shown in Figures 1c–e. Two different fracture sizes were evaluated in all cases. For linear fracture modeling, fracture widths 1 mm and 3 mm widths were tested. For diastatic fractures, fracture widths 4 mm and 6 mm were evaluated. For depressed fractures, fracture diameters 20 mm and 40 mm were simulated. These simulation scenarios consider skull fractures without skin injury since such fractures are more challenging to detect.

In the evaluations, scattering parameter S21, i.e. the channel transfer functions, i.e., were evaluated between the antennas positioned near the head model, simulating their placement in a portable device. S21 parameters were evaluated in both the reference case (a model without skull fractures) and various fracture cases. This sub study provides research output addressing RQ1. The simulations were carried out for the frequency range 2.5–10 GHz to observe the impact of the different fracture types at different frequencies, addressing RQ2. The impact of skull fractures was evaluated and compared using two head layer models with different scalp thicknesses. This comparison aimed to understand how scalp thickness affects the detectability of skull fractures, providing research output for RQ3.

Antenna model

In this study, a flexible monopole antenna is use which is intended for in-body sensing within the 2 – 10 GHz frequency range, encompassing both the ISM band at 2.5 GHz and UWB from 3.1 to 10.6 GHz. This antenna was also employed in prior research on the detection of linear skull fractures [17]. It is constructed on a thin, flexible Rogers5880 substrate and is designed to be attached to the skin surface. Figure 1f illustrates the simulation model

Table 2. Head tissue thickness in head simulation models.

Head model	Head tissue thickness [mm]			
	Skin	Fat	Skull	Dura
Model 1	1.5	1.5	6	1
Model 2	2	3	6	1

of the antenna. The dimensions of the antenna are x = 40 mm, y = 40 mm, z = 0.125 mm, h1 = 11mm, h2 = 10 mm, h3 = 9.1 mm, w1 = 5.7 mm, w2 = 3.8 mm. The antennas were positioned in the simulation model above the head, representing the configuration of a portable or wearable monitoring device with embedded antennas.

Results

In this section, the potential of microwave technique in detecting the most common skull fracture types is evaluated with two different head models having different skin and fat layer thicknesses. Firstly, the impact of the linear fractures is evaluated as the continuation of the studies in [17].

First, the impact of linear fracture having widths 1 mm (Frac.1) and 3 mm (Frac.2) are evaluated. Figures 2a–b illustrates S21 results in the reference case (green line) and in the presence of linear fractures obtained using the Model 1, having thinner scalp (2a), and Model 2, having thicker scalp (2b). The fractures are clearly visible with both models at most of the frequencies within simulated frequency range. Obviously, the differences are clearly visible with the Model 1 having thinner scalp: maximum 5 dB difference at frequencies 3 GHz and 9.5 GHz. As discussed in [17], the impact of the fracture may decrease or increase S-parameters depending on the frequency and also the location of the fracture respect to the antenna. In several cases, the changes are logical: the larger the fracture, the larger the impact is on the results. The difference between S21's obtained with Frac.1 and Frac.2 is small, though still visible.

Next, the impact is evaluated with diastatic fractures having widths 4 mm and 6 mm. The results are presented in Figures 2c–d obtained using Model 1 and Model 2, respectively. With diastatic fractures, the differences between the reference and fractured responses are naturally larger since the fractures are wider than linear fractures. Differences are visible throughout the whole frequency band; the largest differences can be seen at 9.5 GHz. However, with the thicker scalp model, the differences are minor which is expected due to the augmented power attenuation associated with increased tissue thickness.

Subsequently, the impact of the depressed skull fractures was evaluated on the scattering parameters. Figures 2e–f illustrate S21 results in the reference case (green line) and in the presence of depressed fractures with widths 20 mm and 40 mm obtained with the Model 1 (2e) and Model 2 (2f). As can be seen, the depressed fracture is clearly visible with both models: the difference between the fracture and the reference case is over 10 dB at 2.5 GHz and 9.5 GHz. With the thinner scalp model, the differences are visible along the whole simulated bandwidth whereas with the thicker scalp model, the differences are the mostly visible only at 2.5 GHz and 9.5 GHz.

Finally, Table 3 summarizes the impact of the different skull fracture types on the S21-parameter results, highlighting the frequency ranges where differences in S21 results due to fractures are most noticeable. It also indicates whether this impact is increasing or decreasing for the S21 response levels and what is the maximum difference to the reference case. With all studied cases, skull fractures are most detectable around 2.5 – 5 GHz and 9.2 – 10 GHz.

The results presented in this paper complement the previously presented findings on the detection of linear skull fractures using microwave technology in [17]. Although detection of linear skull fractures is most challenging due to their small size, it is essential to understand how also other skull fracture types would affect the channel responses.

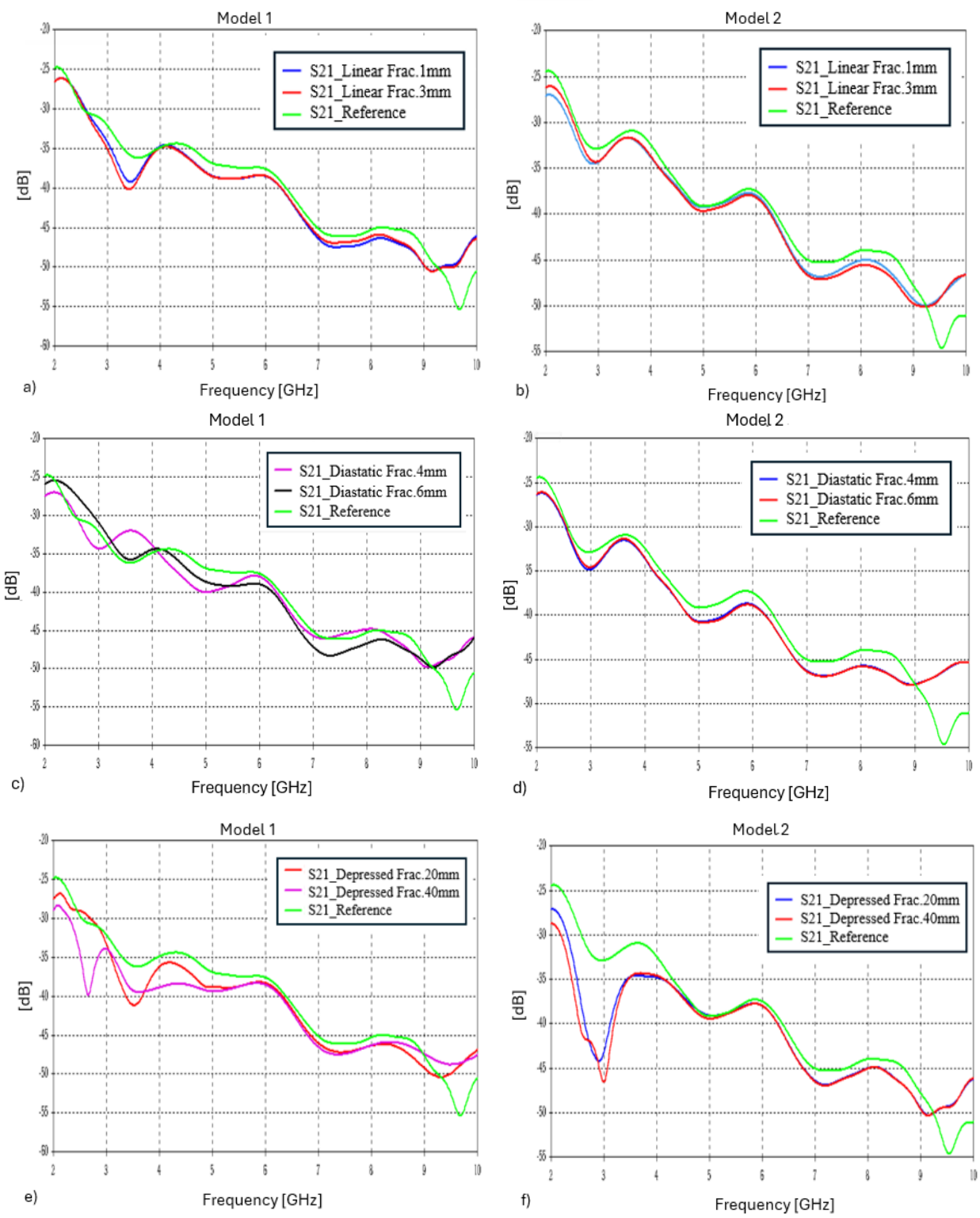

Figure 3. S21 channel parameter evaluations with the head model having thinner scalp (figures on the left) and thicker scalp (figures on the right) in the reference and fractured in the cases: a-b) linear skull fractures, c-d) diastatic skull fractures, and e-f) depressed skull fractures.

Table 3. Impact of skull fractures at different frequency ranges.

Fracture type Head model	Linear Freq. ranges [GHz]	Max. difference [dB]	Diastatic Freq. ranges [GHz]	Max. difference [dB]	Depressed Freq. ranges [GHz]	Max. difference [dB]
Model 1	2.5–3.75 8–9.4 9.5–10	-4 -3 +5	4–6 7–9 9.2–10	-4 -3 +7	2–5.5 9.2–10	-5 +7
Model 2	2.5–4 7–9.2 9.2–10	-2 -3 +6	3–6 7–9 9–10	-2 -3 +7	2–4.2 7–9 9.2–10	-12 -2 +7

Discussion

Recent studies have shown that microwave technique has great potential for detecting tissue abnormalities in various applications, including the detection of linear skull fractures. This paper presented simulation-based evaluations of microwave-based detection for three most common skull fracture types: linear, diastatic, and depressed, using two head models with varying scalp thicknesses. The results are promising: the microwave technique effectively detected all fracture types in both models, with the most significant impacts observed within consistent frequency ranges. Due to brevity, this paper focused on presenting only the simulated S21-parameter results. However, the detectability can be further improved with more sophisticated analysis methods in different domains [22–25] as well as minimizing antenna coupling e.g. through the Multistatic Data Matrix (MDM) approach [26]. Additionally, the microwave technique can employ antenna reflection coefficients (S11 and S22) to detect tissue abnormalities. However, as demonstrated in [17], skull fractures have a more pronounced impact on S21 parameters. Therefore, due to brevity, the analysis of antenna reflection coefficients is omitted from this paper.

This study introduces several novel aspects compared to previous research on microwave-based skull fracture detection. Unlike earlier studies that focused solely on linear fractures, this paper examines the impact of various skull fracture types on scattering parameters using realistically shaped models. Additionally, it provides new assessments of the most promising frequency ranges for skull fracture detection within the ISM and UWB spectrum using a flexible UWB antenna covering these frequency bands. Furthermore, this study uniquely evaluates how scalp thickness affects the detectability of fractures, an aspect not considered in prior research.

Our approach was testing the initial potential of microwaves to detect different types of skull fractures in a simulated environment. It is important to note that a skull fracture is not directly related to the patient's injuries. A patient can have significant intracranial bleeding without a fracture, so ruling out a fracture does not provide a sense of security. Nevertheless, the presence of a fracture indicates a higher energy impact in the injury formation and thus emphasizes the importance of further investigations (primarily CT, also MRI). Similarly, the method is valuable if it can distinguish high energy, e.g. depressed fractures from others. Additionally, microwave technique has also demonstrated

potential in detecting brain hemorrhages using a helmet type of device in several studies [5–6, 27]. However, before assessing possible brain hemorrhages using this technique reliably, it is essential to understand how skull fractures affect the measured scattering parameters. Our next study will focus on investigating the simultaneous presence of skull fractures and brain hemorrhages using realistic simulation and emulation platforms [28]. This research aims to understand the combined impact of these conditions on scattering parameters, which is crucial for improving the accuracy of microwave-based diagnostic techniques.

The previous studies on the detection of linear fractures, as reported in [17], indicate that the microwave technique can detect fractures as narrow as 1 mm. This capability applies to both fresh fractures and those in the healing process. For future development, one direction is to include more detailed study on spatial recognition as well as imaging of the fractures [5, 6, 11]. This would improve the capabilities to monitor the healing process and compare the results with current diagnostic methods based on imaging. Additionally, future work could involve a more comprehensive examination of broader factors, such as inconsistencies in antenna placement and the impact of hair and sweat, to further enhance the practical applicability of the findings.

A portable skull fracture monitoring device which could carry out skull fracture screening as a point-of-care diagnostics type of device e.g., in ambulance or in smaller healthcare centers, could significantly streamline the patient's journey to treatment as a novel telemedicine's application. The device could also facilitate remote consultations regarding a patient, for instance, enabling communication between a health center and the neurosurgery department of a university hospital. Moreover, a device that enables frequent and safe monitoring of skull fracture healing, even in smaller healthcare centers, would be instrumental in identifying potential issues at an early stage. Devices utilizing microwave technology could easily integrate antenna sensors into portable or wearable formats, making them user-friendly. In this study scenario, the antennas are located side by side as in a small handheld portable device which could be moved around the head to detect possible skull fractures or to monitor the healing process of the fractures. Alternatively, a wearable helmet-type device could be advantageous for providing comprehensive analysis to detect fractures throughout the entire skull. Furthermore, this technique supports non-contact sensing, which is particularly beneficial for monitoring fractures in small children [29].

Conclusions

This paper presented simulation-based evaluations of microwave-based skull fracture detection with the most common skull fracture types: linear, diastatic, and depressed fractures. In the simulations, two different head models resembling different scalp thicknesses were utilized. The evaluated scattering parameter results are encouraging: The microwave technique effectively detects various fracture types in both head models, with the impact of the fractures being most pronounced within the same frequency ranges. Based on the objectives and research questions of this study, the following conclusions can be drawn:

1. Different skull fracture types affect the scattering parameters clearly: the larger the fracture, the larger is the impact in channel response.

2. Based on this study, the most optimal frequencies for skull fracture detection are 3 – 5 GHz and 9 GHz.

3. Human scalp thickness affects the detectability of skull fractures slightly. However, even with thicker head tissue model, the fractures are detectable.

Acknowledgements

This research is funded by Academy of Finland Profi6 funding, 6G-Future Sustainable Society (grant 318927), 6GBRIDGE - Next generation healthcare and wearable diagnostics utilizing 6G (11146/31/2022), and InfoTechOulu, which are greatly acknowledged.

Conflict of interest

The authors declare no conflicts of interest.

References

[1] Thomas B, de Castro I, Pait G. Skull Fractures: Classification and Management. Contemp. Neurosurg. 2001;23(17)1-7.

[2] Liew YM, Ooi JH, Azman RR, Ganesan D, Zakaria MI, Mohd Khairuddin AS, Tan LK. Innovations in detecting skull fractures: A review of computer-aided techniques in CT imaging. Phys Med. 2024 Aug;124:103400. doi: 10.1016/j.ejmp.2024.103400.

[3] Alexandridis G, Verschuuren EW, Rosendaal AV, Kanhai DA. Evidence base for point-of-care ultrasound (POCUS) for diagnosis of skull fractures in children: a systematic review and meta-analysis. Emerg Med J. 2022 Jan;39(1):30-36. doi: 10.1136/emermed-2020-209887.

[4] Dehbozorgi A, Mousavi-Roknabadi RS, Hosseini-Marvast SR, Sharifi M, Sadegh R, Farahmand F, Damghani F. Diagnosing skull fracture in children with closed head injury using point-of-care ultrasound vs. computed tomography scan. Eur J Pediatr. 2021 Feb;180(2):477-484. doi: 10.1007/s00431-020-03851-w.

[5] Origlia C, Rodriguez-Duarte DO, Tobon Vasquez JA, Bolomey JC, Vipiana F. Review of Microwave Near-Field Sensing and Imaging Devices in Medical Applications. Sensors (Basel). 2024 Jul 12;24(14):4515. doi: 10.3390/s24144515.

[6] Chandra R, Zhou H, Balasingham I, Narayanan RM. On the Opportunities and Challenges in Microwave Medical Sensing and Imaging. IEEE Trans Biomed Eng. 2015 Jul;62(7):1667-82. doi: 10.1109/TBME.2015.2432137.

[7] Särestöniemi M, Myllymäki S, Reponen J, Myllylä T. Remote diagnostics and monitoring using microwave technique - Improving healthcare in rural areas and in exceptional situations. FinJeHeW. 2023;15(1):6–22. https://doi.org/10.23996/fjhw.122743

[8] Redzwan S, Asan N, Velander J, Lee D, Perez MD, Raaben M, Blokhuis T, Augustine R. Frequency domain analysis of hip fracture using microwave Split Ring Resonator sensor on phantom model. In: 2016 IEEE Asia-Pacific Conference on Applied Electromagnetics (APACE), Langkawi, Malaysia, 11–13 December 2016. p. 244–247. https://doi.org/10.1109/APACE.2016.7916434

[9] Lee D, Shaker G, Augustine R. Preliminary Study: Monitoring of Healing Stages of Bone Fracture utilizing UWB Pulsed Radar Technique. In: 2018 18th International Symposium on Antenna Technology and Applied Electromagnetics (ANTEM), Waterloo, ON, Canada, 19–22 August 2018. p. 1–2. https://doi.org/10.1109/ANTEM.2018.8572872

[10] Santos KC, Fernandes CA, Costa JR. A study on the sensitivity of micro-wave imaging for detecting small-width bone fractures. In: 2021 15th European

Conference on Antennas and Propagation (EuCAP), Dusseldorf, Germany, 22–26 March 2021. p. 1–4. doi: 10.23919/EuCAP51087.2021.9411065

[11] Santos KC, Fernandes CA, Costa JR. Experimental evaluation of thin bone fracture detection using microwave imaging. In: 2022 16th European Conference on Antennas and Propagation (EuCAP), Madrid, Spain, 27 March–1 April 2022. p. 1-3, doi: 10.23919/EuCAP53622.2022.9769388.

[12] Akdoğan V, Özkaner V, Alkurt FÖ, Karaaslan M. Theoretical and experimental sensing of bone healing by microwave approach. Int J Imaging Syst Technol. 2022;32(1):2255–2261. DOI:10.1002/ima.22775

[13] Lee D, Kim K, Augustine R. Monitoring of the skull healing within layered head model based on transmission line theory. In: 2017 First IEEE MTT-S International Microwave Bio Conference (IMBIOC) 2017 First IEEE MTT-S International, Gothenburg, Sweden, 15-17 May 2017. p. 1–3. doi: 10.1109/IMBIOC.2017.7965775.

[14] Lee D, Nowinski D, Augustine R. A UWB sensor based on resistively-loaded dipole antenna for skull healing on cranial surgery phantom models. Microw Opt Technol Lett. 2018;60(4):897-905. https://doi.org/10.1002/mop.31077

[15] Ebrahimi-Zadeh J, Perez MD, Augustine R. Electromagnetic Time-Reversal Technique for Monitoring Skull Healing Stages. In: 2019 13th European Conference on Antennas and Propagation (EuCAP), Krakow, Poland, 31 March–5 April 2019. p. 1–5.

[16] Perez MD, Thomas G, Shah SRM, Velander J, Asan NB, Mathur P, Nasir M, Nowinski D, Kurup D, Augustine RD. Preliminary Study on Microwave Sensor for Bone Healing Follow-up after Cranial Surgery in Newborns. In: 2018 EUCAP 12th European Conference on Antennas and Propagation, London, UK, 9–13 April 2018. p. 1-5. doi: 10.1049/cp.2018.1250.

[17] Särestöniemi M, Singh D, von Und Zu Fraunberg M, Myllylä T. Microwave Technique for Linear Skull Fracture Detection-Simulation and Experimental Study Using Realistic Human Head Models. Biosensors (Basel). 2024 Sep 6;14(9):434. doi: 10.3390/bios14090434.

[18] IT'IS Foundation. IT'IS Foundatio; 2024 [cited 1 April 2024]. Available from: https://itis.swiss/virtual-population/tissue-properties/database/

[19] Bahney CS, Zondervan RL, Allison P, Theologis A, Ashley JW, Ahn J, Miclau T, Marcucio RS, Hankenson KD. Cellular biology of fracture healing. J Orthop Res. 2019 Jan;37(1):35-50. doi: 10.1002/jor.24170.

[20] Orfanidis SJ. Electromagnetic Waves and Antennas. 2002, Revised 2016 [cited on 5 May 2022]. Available from: http://leipper.org/manuals/zipfill/www.ece.rutgers.edu/~orfanidi/ewa/

[21] Dassault Systèmes. Dassault Simulia CST Suite. Dassault Systèmes [cited on 6th June 2022]. Available from: https://www.3ds.com/.

[22] Yamada A, Teramoto A, Otsuka T, Kudo K, Anno H, Fujita H. Preliminary study on the automated skull fracture detection in CT images using black-hat transform. In: 2016 38th Annual International Conference of the IEEE Engineering in Medicine and Biology Society (EMBC), Orlando, FL, USA, 16-20 August 2016. p. 6437–6440. doi: 10.1109/EMBC.2016.7592202.

[23] Chowdhury AS, Bhandarkar SM, Robinson RW, Yu JC, Liu T. Detection of hairline mandibular fracture using max-flow min-cut and Kolmogorov-Smirnov distance. In: 2011 IEEE International Symposium on Biomedical Imaging: From Nano to Macro, Chicago, IL, USA, 30 March–2 April 2011. p. 1962–1965. DOI:10.1109/ISBI.2011.5872794

[24] Lan X, Mo H, Chen S, Liu Q, Deng Y. Fast transformation from time series to visibility graphs. Chaos. 2015 Aug;25(8):083105. doi: 10.1063/1.4927835.

[25] Ebrahimi-Zadeh J, Dehmollaian M, Mohammadpour-Aghdam K. Electromagnetic time-reversal imaging of pinholes in pipes. IEEE Trans. Antennas Propag. 2016;64(4):1356–1363. doi: 10.1109/TAP.2016.2526043.

[26] Zadeh JE, Balegh H, Fallahi R. Electromagnetic DORT time reversal dielectric spectroscopy. In: 2016 8th International Symposium on Telecommunications (IST), Tehran, Iran, 27–28 September 2016. p. 437–441.

[27] Guo L, Alqadami ASM, Abbosh A. Stroke Diagnosis Using Microwave Techniques: Review of Systems and Algorithms. IEEE Journal of Electromagnetics, RF and Microwaves in Medicine and Biology. June 2023;7(2):122-135. https://doi.org/10.1109/JERM.2022.3227724

[28] Särestöniemi M, Singh D, Dessai R, Heredia C, Myllymäki S, Myllylä T. Realistic 3D Phantoms for Validation of Microwave Sensing in Health Monitoring Applications. Sensors. 2024;24(6):1975. https://doi.org/10.3390/s24061975

[29] Sun Q, Shi Y, Zhang F. Pediatric skull fractures and intracranial injuries. Exp Ther Med. 2017 Sep;14(3):1871-1874. doi: 10.3892/etm.2017.4715.

Appendix

This appendix presents the dielectric properties (relative permittivity and conductivity) of head tissues. These values are at various evaluated frequencies are presented in Table A1 [18]. Additionally, the dielectric properties of blood, and connective tissue, which are used to model fresh fracture (blood) and fracture in healing process (connective tissue) are presented. Table A1 also highlights the differences between bone and blood at these frequencies.

Table A1. Dielectric properties of head tissues, blood (modelling fresh fracture) and connective tissue (modelling fracture in healing process) [18].

Tissue	Frequency			
	2 GHz	4 GHz	6 GHz	8 GHz
Skin	38.6	36.6	34.9	33.2
Fat	5.33	5.12	4.84	4.46
Bone	11.6	10.5	9.6	8.8
Blood	59.0	55.6	52.2	48.6
Connective tissues	43.9	40.2	36.4	32.7
Difference between blood and bone	47.4	45.1	42.6	39.8
Difference between connective tissue and bone	32.2	29.7	26.8	23.7